Molecular Crystals and Liquid Crystals

Publication details, including instructions for authors and subscription information:
http://www.tandfonline.com/loi/gmcl20

Characterization of Apatite and Collagen in Bone with FTIR Imaging

H. Kimura-Suda [a], M. Kajiwara [b], N. Matsumoto [b], H. Murayama [b] & H. Yamato [b]

[a] PerkinElmer Japan Co. Ltd., Godo-cho, Hodogaya-ku, Yokohama, Japan

[b] Kureha Special Laboratory Co. Ltd., Hyakunin-cho Shinjyuku-ku, Tokyo, Japan

Version of record first published: 26 May 2010

To cite this article: H. Kimura-Suda, M. Kajiwara, N. Matsumoto, H. Murayama & H. Yamato (2009): Characterization of Apatite and Collagen in Bone with FTIR Imaging, Molecular Crystals and Liquid Crystals, 505:1, 64/[302]-69/[307]

To link to this article: http://dx.doi.org/10.1080/15421400902942144

Mol. Cryst. Liq. Cryst., Vol. 505, pp. 64/[302]–69/[307], 2009

ISSN: 1542-1406 print/1563-5287 online
DOI: 10.1080/15421400902942144

Taylor & Francis
Taylor & Francis Group

Characterization of Apatite and Collagen in Bone with FTIR Imaging

H. Kimura-Suda[1], M. Kajiwara[2], N. Matsumoto[2], H. Murayama[2], and H. Yamato[2]
[1]PerkinElmer Japan Co. Ltd., Godo-cho, Hodogaya-ku, Yokohama, Japan
[2]Kureha Special Laboratory Co. Ltd., Hyakunin-cho Shinjyuku-ku, Tokyo, Japan

We characterize hydroxylapatite and collagen by Fourier transform infrared (FTIR) imaging and light microscopy in different aged rats to investigate bone formations. The proximal tibias from male rats aged between fetus and postnatal 33 weeks were embedded and sliced to make longitudinal sections. FTIR images of amide I distribution in the sections are coincident with the images of Goldner's stained-sections. FTIR images of hydroxylapatite indicate calcification of rat bones can be observed until postnatal 33 weeks at least. It is found for fetus that hypertrophic chondrocyte in perichondrium and bone collar are initially calcified and have poorly ordered hydroxylapatite crystallites.

Keywords: bone; calcification; collagen; FTIR; FTIR imaging; hydroxylapatite

INTRODUCTION

Bone consists of about 45–70 wt% mineral formed mostly of calcium phosphate (hydroxylapatite), 10 wt% water, and the remainder organic materials consisting principally type I collagen with smaller amounts of noncollagenous proteins and lipids [1]. The mineral in bone is located primarily within the collagen fibril, and during mineralization the fibril is formed first and the water within the fibril is replaced with mineral [2]. While bone is a chemical reservoir for phosphorous,

Hiromi Kimura-Suda thanks Mr. Akihiro Ohnishi for technical supports of FTIR analysis.

Address correspondence to H. Kimura-Suda, PerkinElmer Japan Co. Ltd., 134 Godo-cho, Hodogaya-ku, Yokohama 240-0005, Japan. E-mail: hiromi.suda@perkinelmer.com

which is a life essential element, bone must possess the physical properties required for the functionality of the tissue, such as structural support [1].

Bone strength and fracture risk are generally assessed by measuring bone mineral density (BMD), however; the mechanical properties of bone are determined not only bone mass, but also by architecture/geometry of the bone and by the intrinsic material properties of the tissue. It is considered that bone strength is determined by 70% bone density and 30% bone quality. Bone quality is defined by at least four factors: (1) the rate of bone turnover; (2) properties of the collagen/mineral matrix; (3) microdamage accumulations; (4) architecture/geometry of trabecular and cortical bone [3].

Fourier transform infrared (FTIR) and Raman spectroscopy can provide molecular structure information about mineralized and non-mineralized connective tissue. In recent years, Boskey [4–10] and Morris [11–16] have succeeded in determination of bone quality with microscopic FTIR, FTIR imaging and Raman spectroscopy without homogenization or stain. The Boskey group has focused on the state of collagen cross-links in bone and characterized nonreducible/reducible collagen cross-link ratio in disease bone matrix with microscopic FTIR and FTIR imaging. The Morris group has characterized micro crack in bone mineral using a newly developed Raman system.

In previous works [17], we have characterized rickets and normal bone by light microscopy and FTIR imaging. Rickets is bone disease, softening of the bone potentially leading to fractures and deformity. Characterization of rickets bone is a prime case to know the structure and functionality of bone as the first step, since our research goal is to understand the mechanism of fibril mineralization. It is believed that the bone troubled rickets is dominated by collagen. Figure 1 shows longitudinal sections of Goldner's stained proximal tibia from mice. We can observe cortical bone, growth plate, and trabecular bone in the normal longitudinal section (a). In the bone troubled with rickets (b), it is difficult to find the growth plate, and both epiphysis and trabecula are stained in red. That is, epiphysis and trabecula in rickets bone are dominated by collage. The FTIR image of amide I distribution, which show the area existing of collagen, is corresponded with the light microscopic image. FTIR spectra extracted from FTIR image indicate that cortical bone troubled with rickets has poorly ordered hydroxylapatite crystallites.

In this work, we characterize CO_3^{2-} and PO_4^{3-} from hydroxylapatite, and amide I from collagen in the different aged rat bone to investigate bone formation by FTIR imaging.

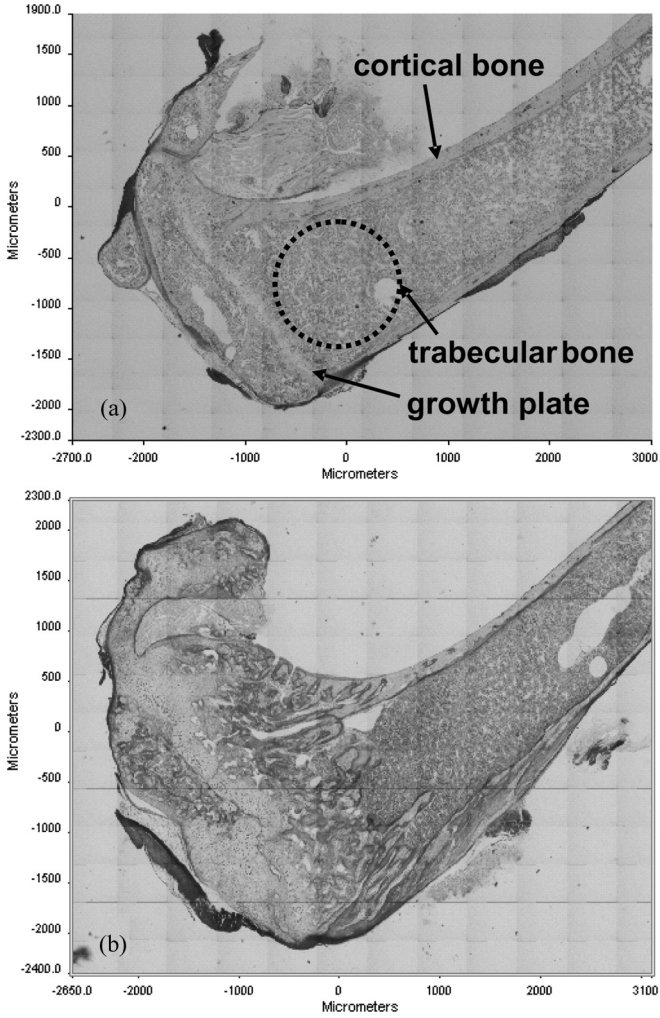

FIGURE 1 Longitudinal sections of Goldner's stained proximal tibia from mice. Normal bone (a) and bone troubled with rickets (b).

EXPERIMENT

Male rats were harvested at different ages; fetal 17 days (unknown sex), postnatal 16 days (P16D), postnatal 6 weeks (P6W), postnatal 12 weeks (P12W), and postnatal 33 weeks (P33W). The proximal tibias from fetus and P16D were frozen, and the tibias from P6 W, P12W and P33W were embedded in PMMA. All specimens were

sliced into 7 μm by microtome to make the two sets of longitudinal sections. A set of sections are mounted on BaF_2 disks for FTIR measurements. Another set of sections are stained with Goldner's trichrome.

FTIR image is acquired by the Spotlight 400 system (PerkinElmer, Inc., MA, USA) with a mercury-cadmium-telluride (MCT) linear array detector. Spectra are corrected using transmittance mode, 2 scans, 4 cm^{-1} resolution, and 25 μm pixel size.

RESULTS AND DISCUSSION

We have compared FTIR images of the longitudinal sections from the different aged rats (P16D, P6W, P12W and P33W). FTIR images of amide I distribution using peptide bond C=O stretch near 1650 cm^{-1}

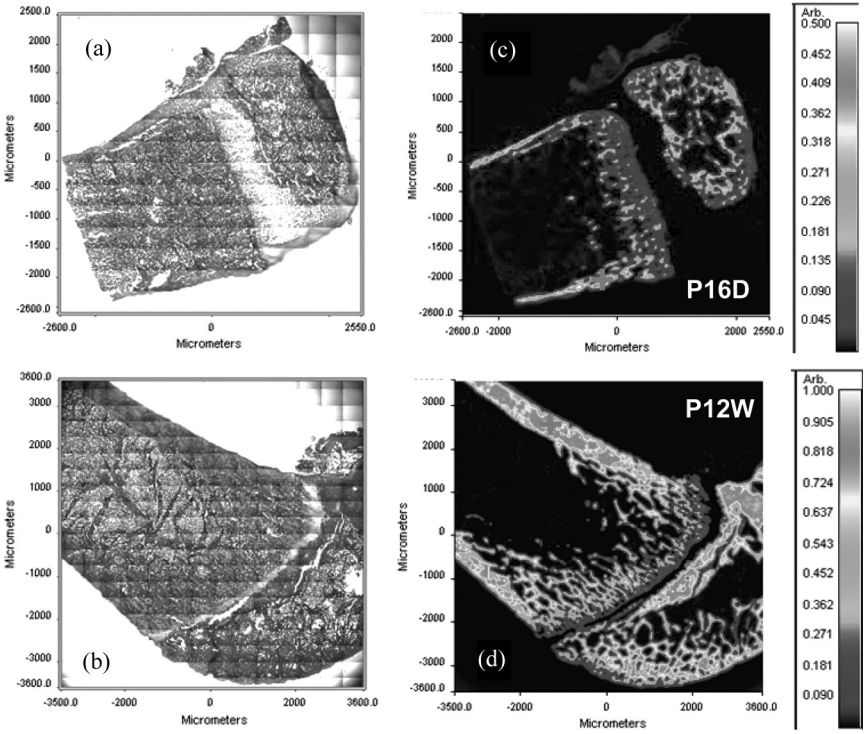

FIGURE 2 Longitudinal sections of proximal tibia from different aged rats. Visible image of P16D (a), visible image of P12W (b), FTIR image of distribution of PO_4^{3-} in P16D (c), and FTIR image of distribution of PO_4^{3-} in P12W (d).

are coincident with the light microscopic images of the sections stained with Goldner's trichrome. FTIR images of PO_4^{3-} band at 1030 cm^{-1}, which is contained in hydroxylapatite, show that hydroxylapatite dramatically increases until postnatal 33 weeks. Figure 2 shows visible images of P16D (a) and P12W (b), and FTIR images of PO_4^{3-} distributions in the same samples, P16D (c) and P12W (d). From postnatal 16 days to 33 weeks, collagen fibril in cortical bone is calcified thicker, and trabecular bone is calcified making network structure during aging. FTIR images of CO_3^{2-} band at 873 cm^{-1}, which replaced OH^- (A-type) or PO_4^{3-} (B-type) in hydroxylapatite lattice, show that carbonate increases as well as phosphate. Figure 3 shows FTIR spectra extracted from marked cortical bone in FTIR images of in P16D and P12W. Amide I, II and II are observed around 1660 cm^{-1}, 1550 cm^{-1}, and 1240 cm^{-1} in both spectra, respectively. In FTIR spectrum of P16D (a), PO_4^{3-} band around 1200–900 cm^{-1} is complex, however; each Amide band is sharp. The PO_4^{3-} band in FTIR spectrum of P33W is sharp. This result indicates that hydroxylapatite crystallites in P16D have a poorly ordered alignment.

We can also observe the calcification of the fetus bone. It is found from FTIR image that hypertrophic chondrocyte in perichondrium and bone collar are initially calcified and have poorly ordered hydroxylapatite crystallites.

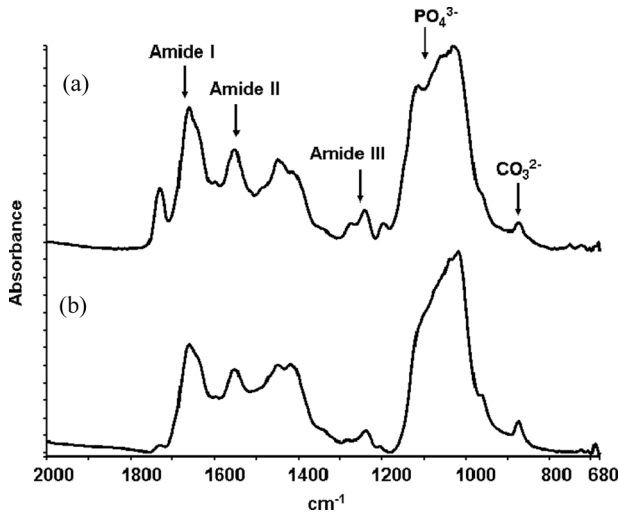

FIGURE 3 FTIR spectra of proximal tibia from different aged rats. FTIR spectrum of cortical bone in P16D (a) and FTIR spectrum of cortical bone in P12W (b).

CONCLUSION

We characterize CO_3^{2-} and PO_4^{3-} from hydroxylapatite, and amide I from collagen in the different aged rat bone to investigate bone formation by FTIR imaging and light microscopy. FTIR images of amide I distribution are coincident with the light microscopic images of Goldner's stained-sections. It is found from FTIR images of PO_4^{3-} that hypertrophic chondrocyte in perichondrium and bone collar are initially calcified, and the calcification of rat bones can be observed until postnatal 33 weeks at least. FTIR spectra indicate that the hydroxylapatite crystallites in P12W have an almost ordered alignment. It may be considered that bone strength of P12W is enough for structural support, since the twelve-week-rat can be bred.

REFERENCES

[1] Skinner, H. (2005). *Biominerals Mineralogical Mag.*, *69*, 621.
[2] Toroian, D. & Price, P. A. (2008). *Calcif. Tissue Int.*, *82*, 116.
[3] Burr, D. B. (2004). *J. Musculoskel Neuron Interact*, *4*, 184.
[4] Paschalis, E. P., Shane, E., Lyritis, G., Skarantavos, G., Mendelsohn, R., & Boskey, A. L. (2004). *J. Bone Miner. Res.*, *19*, 2000.
[5] Paschalis, E. P., Burr, D. B., Mendelsohn, R., Hock, J. M., & Boskey, A. L. (2003). *J. Bone Miner. Res.*, *18*, 769.
[6] Camacho, N. P., Rinnerthaler, S., Paschalis, E. P., Mendelsohn, R., Boskey, A. L., & Fratzl, P. (1999). *Bone*, *25*, 287.
[7] Paschalis, E. P., Boskey, A. L., Kassem, M., & Eriksen, E. F. (2003). *J. Bone Miner. Res.*, *18*, 955.
[8] Atti, E., Gomez, S., Wahl, S. M., Mendelsohn, R., Paschalis, E., & Boskey, A. L. (2002). *Bone*, *31*, 675.
[9] Boskey, A. L. & Mendelsohn, R. (2005). *Vibrational Spectroscopy*, *38*, 107.
[10] Paschalis, E. P., Verdelis, K., Doty, S. B., Boskey, A. L., Mendelsohn, R., & Yamauchi, M. (2001). *J. Bone Miner. Res.*, *16*, 1821.
[11] Carmejane, O. D., Morris, M. D., Davis, M. K., Stixrude, L., Tecklenburg, M., Rajachar, R. M., & Kohan, D. H. (2005). *Calcif. Tissue Int.*, *76*, 207.
[12] Timlin, J. A., Carden, A., & Morris, M. D. (1999). *Appl. Spectrosc.*, *53*, 1429.
[13] Tarnowski, C. P., Ignelzi, M. A., Wei, W., Taboas, J. M., Goldstein, S. A., & Morris, M. D. (2004). *J. Bone Miner. Res.*, *19*, 64.
[14] Tarnowski, C. P., Ignelzi, M. A., & Moriss, M. D. (2002). *J. Bone Miner. Res.*, *17*, 1118.
[15] Crane, N. J., Morris, M. D., Ignelzi, M. A., & Yu, G. (2005). *J. Biomed. Opt.*, *10*, 031119.
[16] Timlin, J. A., Carden, A., & Morris, M. D. (2000). *Anal. Chem*, *72*, 2229.
[17] Kimura-Suda, H., Ohnishi, A., & Yamato, H. (2008). *57th SPSJ Annual Meeting Polymer Preprints*, *57*.